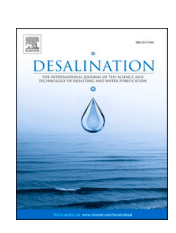
ELSEVIER

Contents lists available at ScienceDirect

Desalination

journal homepage: www.elsevier.com/locate/desal





Photovoltaic powered operational scale Membrane Capacitive Deionization (MCDI) desalination with energy recovery for treated domestic wastewater reuse

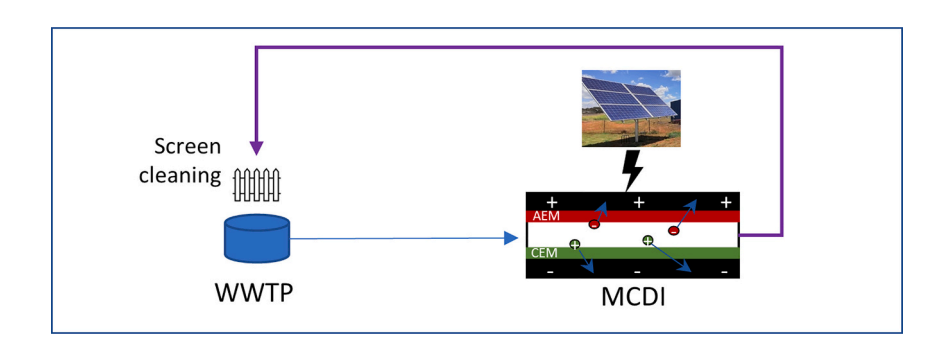
Clare Bales ^a, Boyue Lian ^a, Yunyi Zhu ^a, Hang Zhou ^b, Yuan Wang ^{a,c}, John Fletcher ^b, T. David Waite ^{a,c,*}

- a Water Research Centre, School of Civil and Environmental Engineering, University of New South Wales, Sydney, NSW 2052, Australia
- ^b School of Telecommunications and Electrical Engineering, University of New South Wales, Sydney, NSW 2052, Australia
- ^c UNSW Centre for Transformational Environmental Technologies, Yixing, Jiangsu 214206, PR China

HIGHLIGHTS

- Operational scale MCDI system trialled for treated wastewater reuse applications.
- No performance decline observed over an operational period of 3 months.
- Use of photovoltaics enabled average power saving of 27 %.
- Energy recovery devices facilitated 40 % reduction in electrode energy consumption.
- Performance trends in bench scale studies shown to translate to larger units.

GRAPHICAL ABSTRACT



ARTICLE INFO

Keywords:
MCDI desalination
Long term performance
Energy recovery
Scaled up trials
Performance optimization

ABSTRACT

An operational scale Membrane Capacitive Deionization (MCDI) desalination system was trialled for water reuse applications in Western NSW, Australia. The 6 electrode module system had an average current efficiency of 74 %, water recovery of 84 % (77 % including pre-treatment) and delivered 1.0 m³/h of treated water with an electrode energy consumption of 0.35 kWh/m³ (including energy recovery) and total energy consumption of 1.28 kWh/m³ (using mains power) or 1.05 kWh/m³ (using photovoltaics to power the electrodes). No performance decline was noted over an operational period of 3 months that included reverse current stopped flow desorption and regular cleaning with sodium hypochlorite. The use of photovoltaics for the electrode power supply enabled an average power saving of 27 %. The inclusion of energy recovery devices on the electrode control system facilitated a 40 % reduction in electrode energy consumption. The system demonstrated that MCDI desalination is a feasible option for treated domestic wastewater reuse and can be easily coupled with photovoltaics supply to the electrodes. As one of the first larger scale MCDI operations, we demonstrate that performance trends found in bench scale studies do translate to larger units, however control constraints of the operational units may require optimisation trade-offs between performance parameters.

https://doi.org/10.1016/j.desal.2023.116647

^{*} Corresponding author at: Water Research Centre, School of Civil and Environmental Engineering, University of New South Wales, Sydney, NSW 2052, Australia. E-mail address: d.waite@unsw.edu.au (T.D. Waite).

C. Bales et al. Desalination 559 (2023) 116647

decline was noted with minor removal of TOC. Using RV discharge, foulants that were attracted to the AEM and had accumulated on the

1. Introduction

Nomenclature			Product collection cut off
		P_{elec}	Electrode power consumption
AEM	Anion exchange membrane	PLC	Programmable logic controller
BW	Brackish water	Q_{elec}	Flowrate passing by the electrodes
CC	Constant current	Q_{prod}	Flowrate of the product water
CDI	Capacitive deionization	$R_{\%}$	Removal percentage
CEM	Cation exchange membrane	RC	Reverse current
c_{feed}	Concentration of the feedstream	RO	Reverse osmosis
c_{prod}	Concentration of the product	RV	Reverse voltage
ĊV	Constant voltage	TDS	Total dissolved solids
EC	Electrical conductivity	TDWW	Treated domestic wastewater
EDR	Electrodialysis reversal	TOC	Total organic carbon
E_{elec}	Electrode charging energy consumption per unit of water	V	Electrode voltage
	produced	V_{min}	Minimum discharging voltage
E_{in}	Electrode charging energy consumption	Vol_{brine}	Volume of the brine produced
E_{out}	Energy available from the electrode during discharging	Vol_{prod}	Volume of the product produced
E_{tot}	Total electrode energy consumption including energy	WR	Water recovery
	recovery per unit of water produced	$z_{equivalent}$	Conversion factor from μS/cm to meq/L
F	Faraday constant	Δt_{charge}	Duration of the charging phase
GW	Groundwater	Δt_{cycle}	Total duration of the cycle
I	Applied current	$\Delta t_{discharge}$	Duration of the discharge phase
IEM	Ion exchange membrane	η	Portion of recoverable energy
LCOW	Levelized cost of water	λ	Current efficiency
MCDI	Membrane capacitive deionization		•

Capacitive Deionization (CDI) is an electrochemical desalination method that is primarily used to treat brackish water for potable or industrial purposes. Ions are removed from a feedstream by the application of an electrical potential and are adsorbed onto porous electrodes [1–4]. The process is cyclical with a charge phase generating a product stream followed by a discharge phase generating a brine stream. Ion exchange membranes (IEMs) can be added to the front surface of the CDI anode and cathode in a variation known as membrane CDI (MCDI) with the presence of the IEMs shown to improve performance [5–7]. Specifically, the membranes prevent the absorption of counter-ions during the desorption phase, reduce the extent of electrode fouling and Faradaic processes [8] and have been shown to be more energy efficient than CDI [3].

A number of recent trials on MCDI have been conducted with treated domestic wastewater [9–12] and the use of CDI and MCDI for recovery of nitrogen and phosphorus has been investigated in several studies [13-18]. In a long term trial of treated domestic wastewater with a 40 electrode pair MCDI stack, Shen et al. [10] found a reduction in charge efficiency from 95 % to 75 % over a five month period of operation with fewer ions adsorbed during each cycle as time progressed. The productivity also decreased from 1.36 to 0.96 L/h.m². This was caused by biofouling of the anion exchange membrane (AEM) and anode and formation of inorganic scale, likely calcium carbonate or calcium sulfate, on the cation exchange membrane (CEM) and cathode. The feed was ultrafiltered wastewater effluent from a membrane bioreactor with an electrical conductivity of approximately 550 $\mu S/cm$ with the MCDI operated in constant voltage (CV) mode at 1.2 V. Chemical cleaning, reverse voltage (RV) discharge or additional pre-treatment to assist with fouling and scaling was recommended [10].

Hassanvand et al. [19] studied the performance of CDI and MCDI units with a feedstream to which the organic compounds alginic acid and humic acid were added and found no fouling of the MCDI system after 18 cycles however also observed minimal removal of total organic carbon (TOC) by the MCDI unit. For the CDI unit, some performance

surface were repulsed during the desorption phase [19] in a manner similar to electrodialysis reversal.

In addition to long term performance stability, energy consumption is a critical aspect of any water treatment technology. In MCDI, energy can be recovered during reverse current (RC) discharge [20] with this demonstrated at bench scale to a supercapacitor [21] and at pilot scale with a single electrode module to a battery [22]. Furthermore, MCDI systems operate at low voltages (< 2 V) and, as such, are well suited to power supply from photovoltaics [23,24].

Pilot-sized larger scale MCDI trials are usually limited to a single or double stack of between 10 and 100 electrode pairs [9–12,25–28]. Studies at a larger operational scale using multiple electrode modules are critical to determining if results presented from bench studies are valid in the field and to understand the nature and extent of any interactions that may be occurring between electrode modules. Additional long term trials with MCDI will further assist the understanding of MCDI performance decline over time and further elucidate operational configurations that assist in minimising scaling and fouling.

In this study, an operational scale MCDI unit, with electrodes powered by photovoltaics, is evaluated for desalination of treated domestic wastewater from the Dubbo wastewater treatment plant in western New South Wales, Australia. This system is one of the largest reported trials to date with six electrode modules (each containing approximately 340 electrode pairs). Performance over time was monitored for the multielectrode module unit with RC discharge and a cleaning regime included. A variety of operational configurations were tested to determine if the large scale unit performs in a similar manner to previously studied laboratory and pilot scale units and to identify any differences that may exist between lab scale units and large field scale units. Energy recovery devices were included with operational parameters varied to test the impact of these parameters on a single electrode module as well as on the overall system energy consumption. As the unit has multiple electrode modules, the impact on energy recovery of interactions between these modules was examined. The impact of the inclusion of photovoltaics to power the electrodes on the overall mains power consumption was examined. Having multiple electrode modules electrically and hydraulically in parallel enabled comparison between the individual electrode module performance and the overall system performance. A comparison of the energy consumption and cost of this pilot unit to other water treatment technologies is included to aid the overall assessment of viability of use of MCDI for reduction in salinity of treated domestic wastewater.

2. Materials and methods

2.1. Operational/experimental setup

Dubbo is a regional town in western NSW that had been experiencing severe drought in the years prior to February 2020 [29]. Water reuse options were being explored by Dubbo Regional Council involving the reuse of treated domestic wastewater for agricultural purposes and industrial use, including reuse at the wastewater treatment plant for intake screen cleaning. The operational scale unit was placed after the Dubbo secondary sewage treatment plant (Supporting Information S1 and S2; Figs. S1, S2 and S3) with the product water recycled to the head of the plant to augment potable water used for screen cleaning and the brine sent to onsite evaporation ponds. The secondary effluent from the sewage treatment plant was pumped through a sand filter, activated carbon filter and 5 µm prefilter into a 1.8 m³ influent tank (Fig. 1 and S4). Water was then pumped using variable speed pumps through another 5 µm filter into an MCDI unit consisting of 6 electrode modules (C-17, Voltea Pty. Ltd., USA). Each electrode module consists of 340 electrode pairs giving an approximate electrode area of 7.5 m². Each electrode module was fitted with an in house designed dc-dc bidirectional converter that supplied power for electrode charging and recovered the energy during electrode discharging [22,30]. The critical parameter for product water quality was for total dissolved solids (TDS) concentration to be less than or equal to the average town potable supply of 250 mg/L [31]. This equates to 0.43 mS/cm (assuming $TDS(mg/L) = 580 \times EC(mS/cm)$ from the average ratio of historical water sampling at the Dubbo wastewater treatment plant).

The system was controlled (either on site or remotely) using a Siemens s7–1200 series programmable logic controller (PLC) [32]. The energy for the electrode modules came from 9×12 V 100 A.hr batteries that could be charged either via mains power or from 6×330 W photovoltaic panels (Jiangsu Green Energy Technology, China).

Modules 1–3 were connected to one battery bank and modules 4–6 were connected to a second battery bank with the current supplied by each of these banks recorded by two LEM DK-B420 B dc current transducers. The battery voltage was recorded at the dc-dc bidirectional converters. Whole of system power consumption was recorded using a Schneider Electric iEM2100 energy meter. For an additional schematic of the electrical system, please refer to the Supporting Information S3 Fig. S4.

The electrodes were operated in constant current (CC) mode to a maximum of 1.5 V with reverse current (RC) stopped flow discharge down to a minimum of 0.2 V (refer to Table 1). A higher current was applied during discharge to reduce discharge time and increase productivity. Stopped flow discharge was used to improve water recovery (WR) [22] and was followed by a brief period with flow and no applied current during which brine was collected (Fig. 2). The average influent electrical conductivity (EC) was 1.16 mS/cm (after pre-treatment) with concentrations of major ions given in Table 2. As there was no disinfection prior to the MCDI unit, a weekly flush with sodium hypochlorite (0.14 mM (10 ppm) for 20 min) was undertaken to prevent biofouling. For data collection each value shown is the average of 4 to 12 h of operation.

Four of the electrode modules demonstrated similar performance whereas two had slightly lower performance, likely due to different hydraulic conditions within the modules leading to an overall lower flowrate through the modules at the same inlet pressure. A lower current was applied to these two lower performing electrode modules during the long term operation studies. The long term operation studies were undertaken using all six electrode modules whereas configuration testing with differing flowrate and applied current was undertaken on the four electrode modules of similar performance.

2.2. MCDI performance testing

In order to maintain a constant feedwater quality, the MCDI system was operated in recycle mode with both the brine and product lines redirected back to the $1.8~{\rm m}^3$ influent tank to enable performance testing of the unit. Operation in recycle mode was undertaken for an initial one and a half month recycle period after which the water was replaced and operation in recycle mode continued for a second month and a half. Impact of daily variations of the feedwater was also assessed by operating the MCDI system under single pass mode for 13 days using water directly from the secondary clarifier. Operational configurations used throughout these trials are provided in Table 1.

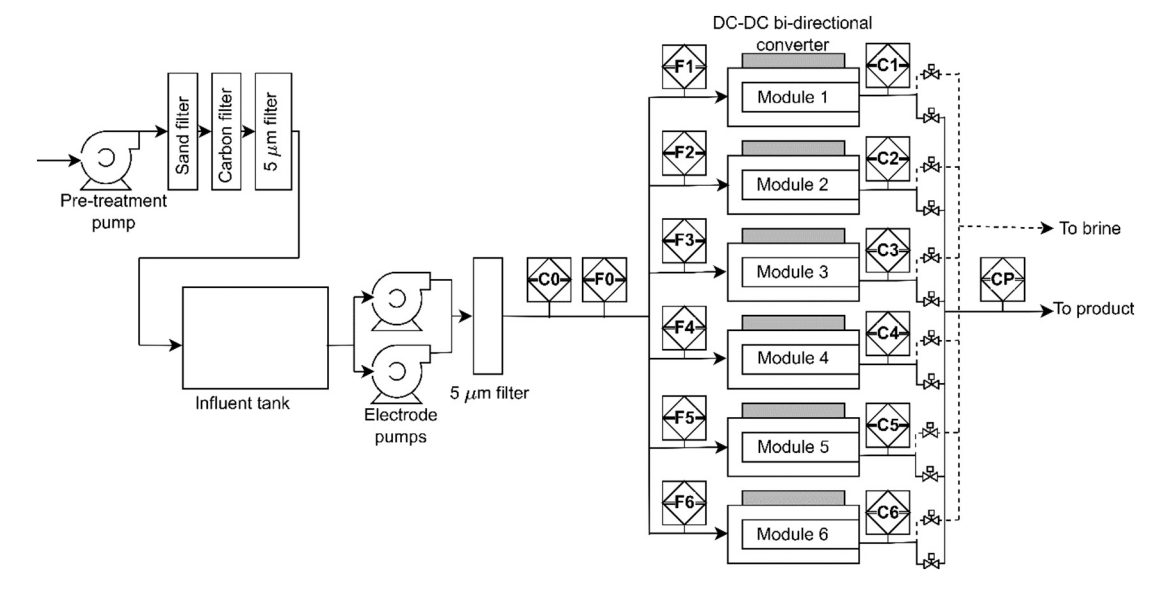


Fig. 1. Schematic of the MCDI unit and pre-treatment system. C0 is the influent EC meter, C1-C6 are the electrode module EC meters and CP is the product EC meter. F0 is the total flowmeter and F1-F6 are the individual electrode module flowmeters. Product and brine solenoid valves are shown.

Table 1 Operational configurations including number of electrode modules, applied current (A) and average electrode module flowrate, Q_{elec} (L/min), for the single pass operation and recycle periods 1 and 2. The electrodes were operated with CC charging up to 1.5 V and RC stopped flow discharging down to 0.2 V.

	Dates	No. electrode modules	Applied current, charging (A)	Reverse current, discharging (A)	Average Q _{elec} (L/min)
Single pass	31/05 to 6/9/21 and 18/11 to 30/11/21	6	$105 \times 4,70,50$	115 × 4, 80, 60	4.1
Recycle period 1	6/10 to 15/11/21				
Long-term operation study		6	$105 \times 4, 70, 50$	$115 \times 4, 80, 60$	6.3
Recycle period 2	15/12/21 to 19/01/22				
Long-term operation study		6	$105 \times 4, 70, 50$	$115 \times 4, 80, 60$	5.0
Flowrate study		4	105	115	3.8 to 7.2
Applied current study		4	90 to 120	110 % charging current	6.1 ^a

^a For the first set of experiments, the average Q_{elec} for the 90 A case was 6.3 L/min, for the 95 A case was 6.5 L/min, for the 100 A case was 6.9 L/min, for the 105 A case was 6.8 L/min, for the 110 A case was 7.1 L/min, for the 115 A case was 6.8 L/min and for the 120 A case was 6.9 L/min. For the set of experiments with an altered product collection cut off, the average Q_{elec} for the 90 A, 95 A and 105 A cases was 5.6 L/min, for the 100 A case was 5.2 L/min and for the 110 A, 115 A and 120 A cases was 5.5 L/min.

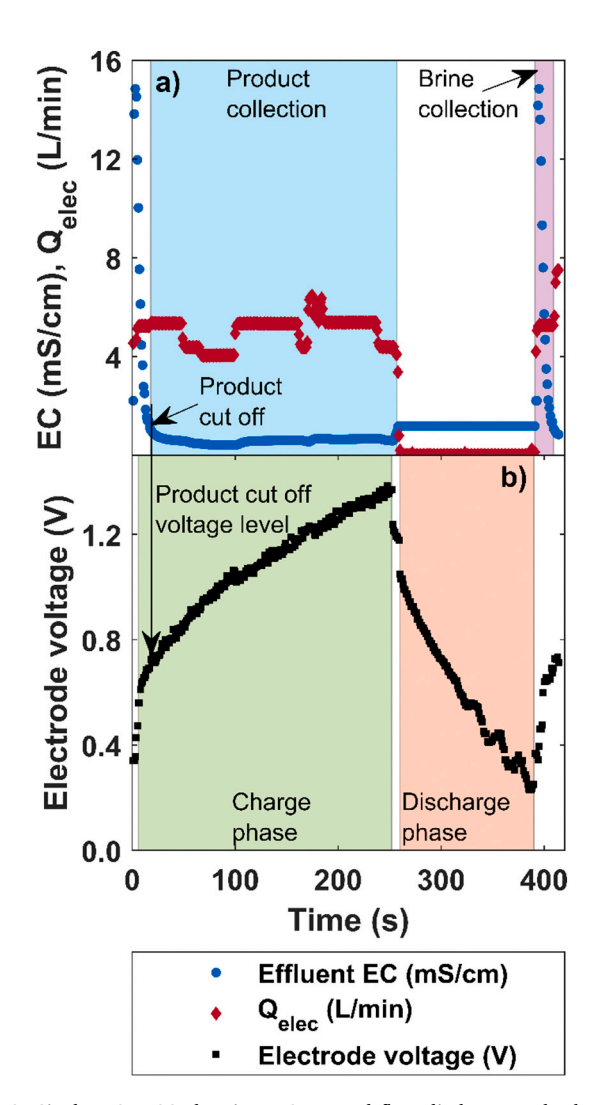


Fig. 2. Single MCDI CC charging, RC stopped flow discharge cycle showing traces for a) effluent EC (mS/cm) and electrode flowrate, Q_{elec} , (L/min) and b) electrode voltage (V). Product collection, brine collection, charging and discharging phases are highlighted. The product cut off and associated product cut off voltage level are shown.

During the second recycle mode period (i.e. from 15/12/21 to 19/01/22) in which the four electrode modules with similar performance were used, tests of differing flowrate and applied current were undertaken to assess whether performance of the operational scale unit

matched that of previously studied bench scale MCDI units. For the varying flowrate cases, the charging current was 105 A and the discharging current was 115 A. For the varying applied current cases, the average flowrate was 6.4 L/min and the discharge current was set to be 10 % higher than the charging current. Refer to Table 1 for operational configuration details. Water sampling was undertaken during both recycle periods (refer Supporting Information S4 for analytical methods). The performance of the energy recovery system was also examined under different minimum discharge voltages.

2.3. Performance metrics

The MCDI performance metrics were calculated using standard methods proposed by Hawks et al. [33]. The flowrate of the product water, Q_{prod} (m³/h), is calculated from:

$$Q_{prod} = \frac{Vol_{prod}}{\Delta t_{cycle}} \tag{1}$$

where Vol_{prod} is the volume of product produced (m³) and Δt_{cycle} is the total cycle duration in hours.

Energy consumption per unit of water produced, E_{tot} (kWh/m³) is given by:

$$E_{tot} = \frac{E_{in} - \eta E_{out}}{Vol_{prod}}$$
 (2)

where:

$$E_{in} = \int_{\Delta l_{cools}} IVdt \text{ where } IV > 0$$
 (3)

$$E_{out} = \left| \int_{\Delta t_{cycle}} IV dt \right| \text{ where } IV < 0 \tag{4}$$

where I is the applied current (A), V is the electrode voltage (V) measured at the electrodes and η is the efficiency of recoverable energy.

For CC mode with a constant applied current E_{in} and E_{out} become:

$$E_{in} = IV_{avg,charge} \Delta t_{charge}$$
 (5)

$$E_{out} = IV_{avg,discharge} \Delta t_{discharge}$$
 (6)

where $V_{avg,charge}$ is the average electrode voltage during charging (V), Δt_{charge} is the duration of the charging phase (hrs), $V_{avg,discharge}$ is the average electrode voltage during discharging (V) and $\Delta t_{discharge}$ is the duration of the discharging phase (hrs).

The power consumption, P_{elec} (kW), was measured so η can be calculated by rearranging Eq. (2) to give:

Table 2
Chemical parameters and removal percentages for cations and anions through the MCDI system at changing flowrate and applied currents. Percentage reductions for a high performance and low performance electrode are also given. SD denotes standard deviation where multiple samples were analysed. RP denotes recycle period when sampling was undertaken. Refer to Supporting Information S4 for chemical analysis methodology.

	Na ⁺	K^+	Ca ²⁺	${\rm Mg}^{2+}$	Cl ⁻	NO_3^-	$\mathrm{SO_4^{2-}}$	P
Feed (before pre-treatment) mg/L (RP 1)	161.6	17.2	3.91	15.0	110.4	4.68	45.3	6.36
Feed (after pre-treatment) mg/L (RPs 1 and	148.4 (SD	14.4 (SD	4.3 (SD 1.1)	14.3 (SD	118.8 (SD	3.9 (SD	45.6 (SD	7.2 (SD 1.5)
2)	11.1)	2.4)		0.8)	21.5)	0.50)	15.6)	
6.1 L/min at 105 A	50 % (SD 5	56 % (SD 2	84 % (SD 11	77 % (SD 3	67 % (SD 11	68 % (SD 15	31 % (SD 22	34 % (SD 11
(RPs 1 and 2)	%)	%)	%)	%)	%)	%)	%)	%)
5.1 L/min at 105 A (RPs 1 and 2)	62 % (SD 15	71 % (SD 23	84 % (SD 2	85 % (SD 1	82 % (SD 0	83 % (SD 4	65 % (SD 4	60 % (SD 5
	%)	%)	%)	%)	%)	%)	%)	%)
4.3 L/min at 105 A (RP 2)	69 %	73 %	93 %	85 %	75 %	76 %	57 %	61 %
6.1 L/min at 90 A (RP 2)	31 %	28 %	88 %	74 %	63 %	68 %	22 %	15 %
6.1 L/min at 100 A (RP 2)	54 %	59 %	90 %	83 %	65 %	69 %	29 %	16 %
6.1 L/min at 110 A (RP 2)	64 %	67 %	90 %	87 %	77 %	78 %	51 %	59 %
6.1 L/min at 120 A (RP 2)	70 %	75 %	97 %	86 %	87 %	89 %	57 %	62 %
High performance electrode at 7.6 L/min at 105 A (RP 1)	64 %	80 %	91 %	80 %	79 %	76 %	45 %	46 %
Low performance electrode at 3.5 L/min at 50 A (RP 1)	39 %	48 %	79 %	60 %	69 %	75 %	77 %	59 %

$$\eta = \frac{\left(E_{in} - \int_{\Delta t_{cycle}} P_{elec} dt\right)}{F}$$
(7)

The electrode charge energy per unit of water produced, E_{elec} (kWh/ m^3) is given by:

$$E_{elec} = \frac{E_{in}}{Vol_{prod}}$$
 (8)

The water recovery, WR, is calculated as:

$$WR = \frac{Vol_{prod}}{Vol_{prod} + Vol_{brine}}$$
 (9)

where Vol_{brine} is the volume of brine produced.

The current efficiency, λ , is dependent on the amount of salt removed, Δc (μ S/cm), the flowrate passing by the electrodes, $Q_{elec}(L/s)$ and I (A) [2,33,34].

$$\lambda = \frac{\Delta c Q_{elec} F_{Z_{equivalent}}}{I}$$
 (10)

where F is the Faraday constant (96,485C/mol) (1 A = 1C/s) and $z_{equivalent}$ converts from μ S/cm to meq/L to account for mol/L and ionic charge, 1.0×10^{-5} used here [35].

The percent removal, R_%, is calculated as follows:

$$R_{\%} = \frac{c_{\text{feed}} - c_{\text{prod}}}{c_{\text{feed}}} \tag{11}$$

where c_{feed} is the concentration of the influent (mg/L, μ S/cm) and c_{prod} is the average concentration of the product (mg/L, μ S/cm).

3. Results and discussion

3.1. MCDI performance

3.1.1. Salt removal, water recovery and current efficiency over long term operation

The MCDI system performance over the two recycle periods was relatively stable (Fig. 3) with an average product EC of 0.43 mS/cm, WR of 84 % and λ of 74 %. During single pass operation, the WR of the pretreatment system was 92 %, resulting in an overall WR of 77 % for single pass. A significant increase in pressure drop over the 5 μ m pre-filter (Supporting Information Figs. S5 and S6) caused a decline in flowrate for the second recycle period (from 6.3 L/min to 5.0 L/min). This is

likely due to the accumulation of biogenic material on the pre-filter that occurred during a warm weather period of non-operation. There was no increase in pressure drop across the electrode modules over the course of the study (Supporting Information Figs. S5 and S6) indicating that there was no significant accumulation of particulate material within the electrode module spacer channels. The accumulation on the pre-filter resulted in a decrease in production rate of the 6 modules, Q_{prod.6}, from 1.14 m³/h to 0.86 m³/h and, as electrode charging energy consumption, Eelec, is a function of Volprod, also resulted in an increase in E_{elec} from 0.53 kWh/m³ to 0.70 kWh/m³. E_{elec} remained stable for the duration of each of the recycle periods. There was an associated decrease in cycle time from period one of 528 s to 463 s in period two however no decline during each period or at an individual electrode module level was evident. When tested at the end of the trial, the TOC of the treated water (at 8.5 mg/L) was slightly higher than that of the feed stream (at 6.5 mg/L). No increase in pressure was noted on the electrode modules, so this increase in TOC is likely due to release of organic material from the pre-filter. There was a decrease in performance after the first day of operation on the second recycle period with this is potentially due the high TOC content of the water. When a new tank of water was supplied for the last two days of testing (18 and 19/01/2022), the current efficiency increased to 82 %, higher than the first recycle period of 74 % (Fig. 3c). If the unit had been operating in single pass mode, these high TOC levels may not have been observed.

When operating in recycle mode, the system was cleaned once per week with 0.14 mM (10 ppm) sodium hypochlorite though under single pass operation the frequency of this clean-in-place process could be reduced. No increase in pressure on the electrodes or performance decline was evident indicating that the frequency of cleaning was adequate (refer Supporting Information S5). Over a five month trial with a 40 pair electrode system, Shen et al. [10] found biofilm growth on the AEM and anode and calcium scaling on the CEM and cathode, however no cleaning regime was included and zero current discharge was used. Results of laboratory scale studies by Hassanvand et al. [19] demonstrated that RC discharge dislodges negatively charged organic compounds from the AEM which would presumably reduce the rate and extent of biofilm growth. The results of the study described here are consistent with these observations though longer term studies are needed to confirm this. The hardness of the feed stream used here was moderate at 70 mg/L (as CaCO₃) with the calcium levels in particular very low at only 4.3 mg/L so inorganic scaling on the CEM and cathode is unlikely to occur under these conditions. Further long term trials using single pass would confirm the operation and maintenance requirements and illuminate any issues with scaling, particularly with the use of stopped flow discharge.

C. Bales et al. Desalination 559 (2023) 116647

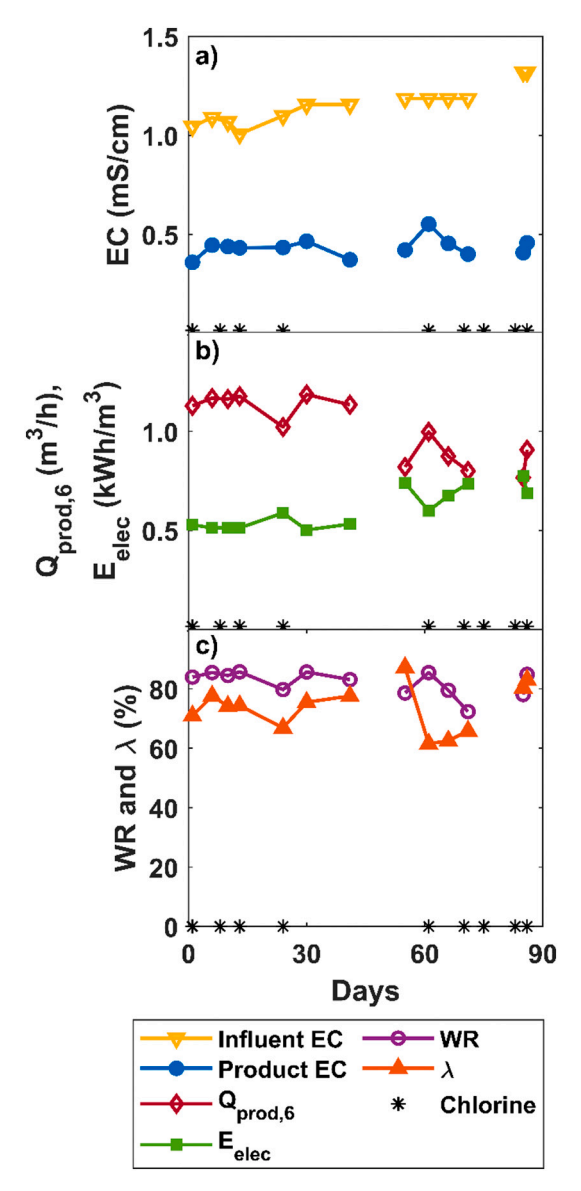


Fig. 3. System performance over 90 days for a) electrical conductivity, b) total flowrate of the product water for 6 electrode modules and average electrode charge energy (no energy recovery accounted for), and c) water recovery and current efficiency. Timing of chlorine wash is denoted as a black star.

By operating with a higher discharge current than charging current compared to operating with equal discharging and charging currents, the $Q_{prod.6}$ increased by 0.005 m^3/h (only 1 %, from 0.717 m^3/h to 0.722 m^3/h), with an increase in λ of 4.1 % (from 66.7 % to 70.8 %) and with minor impacts on other performance indicators including increase in E_{elec} from 0.652 kWh/m³ to 0.658 kWh/m³, decrease in product EC (0.03 mS/cm, from 0.49 μ S/cm to 0.46 μ S/cm) and decrease in WR of 0.8 % (from 87.1 % to 86.3 %). In view of these findings, we are of the view that operating with higher discharge current is not advantageous given the more complex control requirements.

3.1.2. Salt removal, water recovery and current efficiency under various flowrate and applied current configurations

In accord with the results from bench scale units [4,33,36–38], the product EC increased as the $Q_{\rm elec}$ increased (Fig. 4a). As expected, $Q_{\rm prod}$ increased and the associated $E_{\rm elec}$ decreased as flowrate increased (Fig. 4b). Also, WR and λ increased as flowrate increased. For MCDI, the switch over between product and brine (product cut off, Fig. 2) can be varied to modify the effluent EC with the cut off typically set to equal the

influent EC [33]. For the pilot-scale unit used here, the cut off setting was programmed to be determined by the electrode voltage rather than effluent EC (i.e. above 0.7 V the effluent was diverted to product and below 0.7 V the effluent was diverted to brine, Fig. 2). For the low flow cases, by keeping the product cut off voltage level constant, the brine was not all expelled in some instances before the product valve was opened (refer product EC for <5 L/min cases in Fig. 4a). When the product collection cut off voltage level was adjusted to compensate, the overall product EC of the low flow cases decreased (Fig. 4d), however the WR and $Q_{\rm prod}$ were reduced (Fig. 4e and f). This demonstrates that as MCDI moves from bench scale to a useful operational scale, optimum system performance will require compromises in view of its relatively complex control requirements and dependencies. In this regard, machine learning has recently been utilised to assist optimisation of MCDI operation [39].

In Fig. 4, the large standard deviation in the product EC is due to two factors; firstly, the operation of the six electrode modules was staggered to ensure that some were charging whilst some were discharging with this done to balance the total flowrate and energy consumption. However, due to variances between the electrode modules, the Δt_{cycle} was not uniform and, as a result, all electrode modules were occasionally charging at the same time or all electrodes were discharging at the same time. When all of the electrode modules were charging at the same time, the Q_{elec} was very low and, when all but one or two were discharging, the Q_{elec} was high with this variation in Q_{elec} causing fluctuations in the in-line product EC measurement. Secondly, higher EC effluent from the end of the brine phase occasionally entered the product stream at the commencement of this operational phase (refer Fig. 2). The standard deviation shown in Fig. 4 includes these fluctuations. Such variations are to be expected for a multi-electrode MCDI trial and were acceptable for this trial where attainment of an average product EC that was below a particular target value was the objective. For an application where less variation is required, the product collection cut off voltage level can be increased to ensure product EC consistency. For $E_{\rm elec}$, λ and WR, the rate of change in voltage increased and the cycle time shortened as the flowrate decreased with the effluent EC exhibiting a truncated or nonexistent steady state period (Fig. 2). This caused increased variability between the cycles. This is particularly noticeable for the cases with an adjusted product cut off voltage level (Fig. 4e and f).

Increasing the applied current resulted in a similar performance change to that observed in studies with bench scale units [2,33,37,38] with a decrease in product EC as applied current increased (Fig. 5a). As can be seen from Fig. 5b and c, WR (average 89 %) and λ (average 67 %) remained relatively stable as applied current increased and, as expected, E_{elec} increased from 0.53 kWh/m³ at 90 A to 0.65 kWh/m³ at 120 A. Anomalies with the variable speed pumps led to interesting results. For example, despite the pump settings remaining constant, the average flowrate during the 90 A and 95 A cases were lower than those observed at the other applied currents studied (6.4 L/min rather than 6.8 L/min), so a direct comparison of salinity reduction is not appropriate. These results highlight the fact that when interpreting results from these larger operational units, consideration of all operating conditions is important.

Once again, the product cut off voltage level was changed to assess whether better performance could be obtained (Fig. 5d, e and f) at high currents. A moderate improvement in product EC was obtained however, as the $\mathrm{Vol}_{\mathrm{prod}}$ per cycle declined, the WR dropped dramatically from 88 % at 120 A with the original product cut off to 46 % for altered product cut off voltage level. $\mathrm{Q}_{\mathrm{prod}}$ decreased with an associated increase in $\mathrm{E}_{\mathrm{elec}}.$ This again shows that when operating larger scale units, compromises are necessary with the flexibility provided by the programmable logic controller (PLC) and the charge/discharge current controllers critical to realising optimal operating conditions.

The large standard deviation of the $E_{\rm elec}$, λ and WR in Fig. 5e and f as the applied current increased is again caused by the enhanced variability due to the increase in the rate of change of voltage during charging and

C. Bales et al. Desalination 559 (2023) 116647

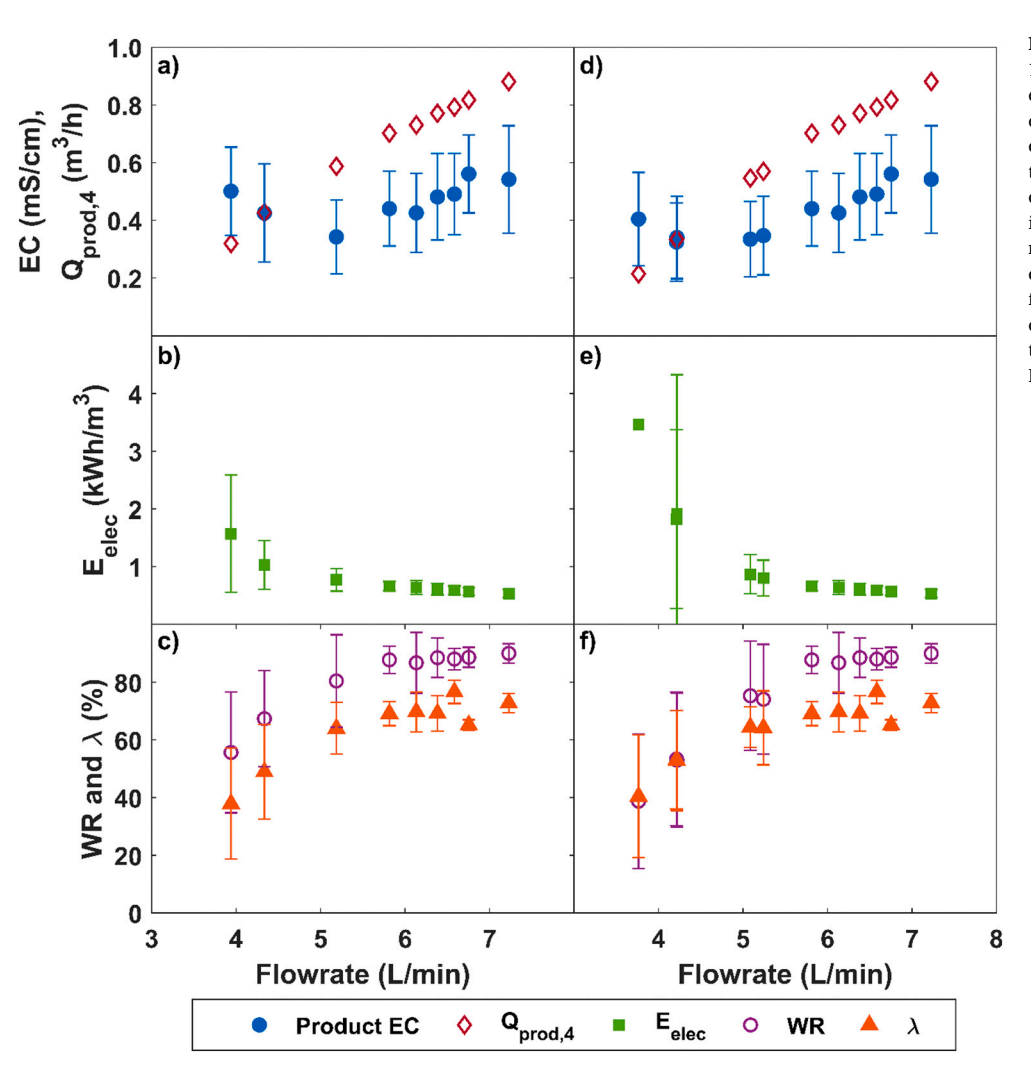


Fig. 4. System performance at influent EC at 1.2 mS/cm for a) and d) product EC, b) and e) total flowrate of the product water for 4 electrode modules and average electrode charge energy (no energy recovery accounted for), and c) and f) water recovery and current efficiency of the MCDI system under increasing flowrate through the electrode module. For a), b) and c), the product collection cut off voltage remained the same for each case. For d), e) and f), the product collection cut off voltage was increased for the <5 L/min cases to improve product EC. Error bars denote standard deviation.

shortened cycle time as the applied current increased. The increase in the rate of change of voltage due to the higher current density caused the product effluent EC to exhibit a truncated or non-existent steady state period.

3.2. Removal of major ions

Results of water quality analyses of the treated stream demonstrated similar trends to previous work with divalent cations exhibiting preferential removal over monovalent cations [9,10] (Table 2). For the anions, the removal of Cl^- and NO_3^- was very similar at 67 % and 68 % respectively for the standard 6.1 L/min at 105 A case. The removal of SO_4^{2-} and PO_3^{3-} through the system was much lower at only 31 % and 34 % for the standard case respectively. Similar results were obtained by others [9,10], with several AEMs preferentially selecting for Cl^- over SO_4^{2-} [40].

For the studies with differing flowrate and applied current, the trends for ion removal also followed the general trend for EC with increasing removal as the flowrate reduces and the applied current increases (Table 2). The removal of SO_4^{2-} and PO_4^{3-} show sensitivity to both flowrate and applied current with only 29 % for SO_4^{2-} and 16 % for PO_4^{3-} removal at 100 A. Kim et al. [9] reported faster migration of Cl^- and SO_4^{2-} through the AEM at higher voltages. Using CC mode, as done in the current study, the rate of change of voltage increases and the electrodes reach high potentials more rapidly with increase in applied current. This higher applied current and subsequent high potentials may be driving faster migration of Cl^- and SO_4^{2-} through the AEM.

The removal percentage of NO_3^- was high with a maximum of 89 % removal (to 0.5 mg/L) at an applied current of 120 A (Table 2). The lowest NO_3^- removal was still 68 % at the applied currents of 90 to 105 A (to 1.7 mg/L). Flowrate did not have as much influence on NO_3^- removal as applied current. Even the low performing electrode at 3.5 L/min with an applied current of 50 A delivered a NO_3^- removal of 75 %.

3.3. Energy consumption

3.3.1. Energy consumption using mains versus photovoltaics

For the long term operation study, the average power and energy requirements for the overall system (including electrode modules, pumps, valves and control system) was 1.31 kW (equivalent to 1.28 kWh/m³) when using mains power supply. The energy for the electrode modules could be supplied via a photovoltaic array and, in this case, the power required for ancillary (including pumps, valves and control system) was 0.95 kW (equivalent to 1.05 kWh/m³). For comparison, the electrodes consumed 27 % of the overall power when they were powered via mains power supply (equivalent to 0.36 kW). As the system is scaled up with additional electrodes, the fixed energy costs associated with the balance of plant (non-electrode module energy consumption) would be expected to become a lower contributor to the total energy consumed and the net benefit of energy recovery and integration with photovoltaics would be expected to offer even better returns. An example projection shows that the two pumps used in the system described could supply (with the same energy consumption) up to 12 electrode modules at 5.7 L/min and 2.5 bar, which would increase the

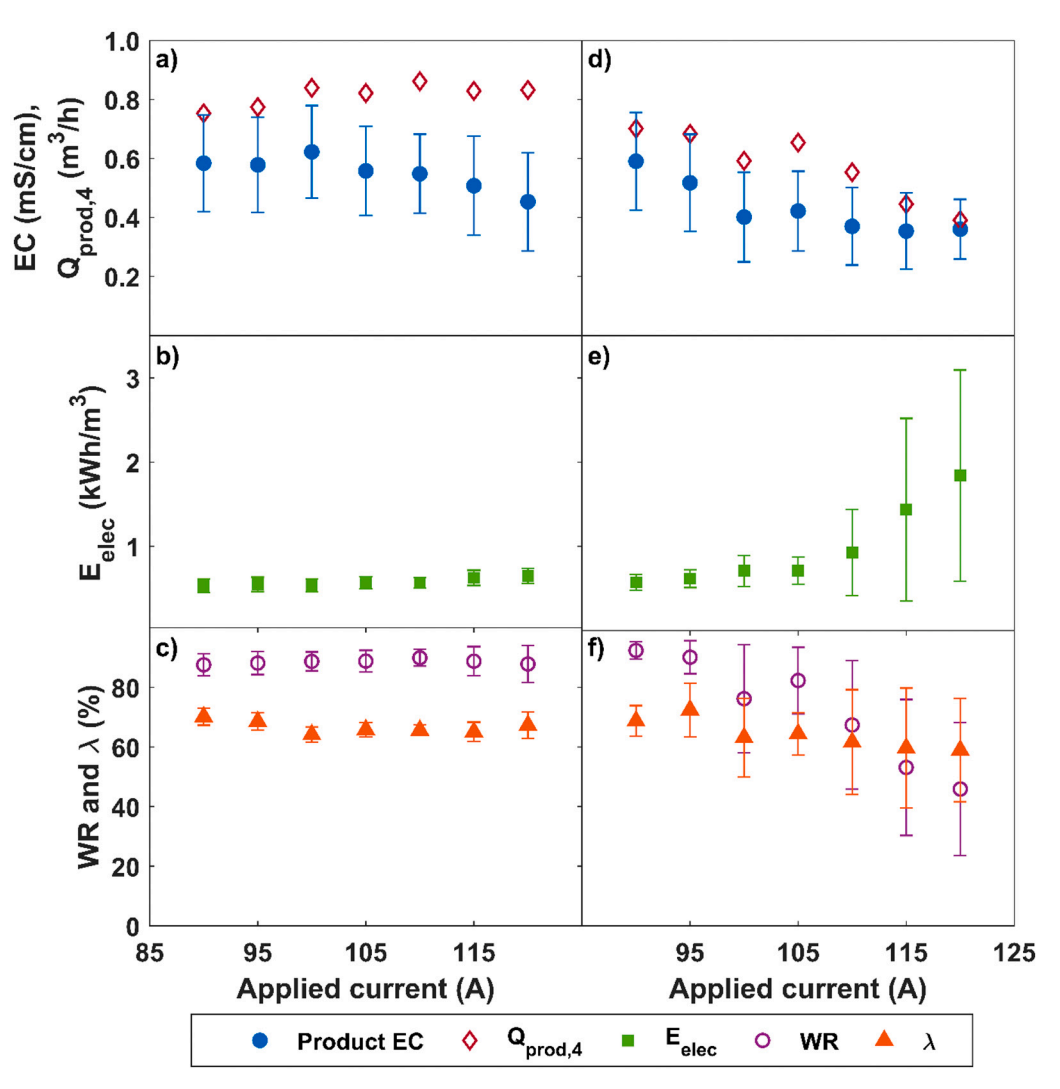


Fig. 5. System performance at influent EC at 1.2 mS/cm for a) and d) product EC b) and e), total flowrate of the product water for 4 electrode modules and average electrode charge energy (no energy recovery accounted for), and c) and f) water recovery and current efficiency of the MCDI system under increasing applied current through the electrode module. For a), b) and c), the product collection cut off voltage remained the same for each case and, for d), e) and f), the product collection cut off voltage was adjusted for all cases to determine if product EC could be lowered. Error bars denote standard deviation.

Table 3
Comparison between this study using operational scale MCDI and other water treatment technologies (RO and EDR) for salinity removal, total system energy consumption and cost of water.

	Influent (mg/L)	$\Delta c \text{ (mg/L)}$	Flowrate of product water (m ³ /d)	Total system energy (kWh/m³)	Cost of water (US\$/m3)a	Reference
RO	BW 2000	1950	4.6	1.1	N/A	Alghoul et al. [44]
RO	TDWW 1461	902-1169	5.0	$0.46-1.22^{a}$	N/A	Hafiz et al. [45]
RO	GW 4000-4500	N/A	50	1.7-1.9	N/A	Peñate et al. [46]
RO	NaCl 1500	1000	379	0.2-0.52	0.12-0.25	Liu et al. [42]
RO	GW 2000	1570	960	N/A	0.24-0.30	Alsarayreh et al. [47]
RO	TDWW 1310	N/A	~2400	0.74-0.83	0.65-0.77	Kehrein et al. [48]
RO	BW 3000	2700	35,000	0.4-0.7	0.22-0.27	Vince et al. [49]
EDR	GW 1600	1300	10	N/A	0.64	Bian et al. [50]
EDR	GW 1300-1500	1050	18.4 ^b	2.67	1.87-3.33	He et al. [51]
EDR	TDWW 1104	776	144	0.6-1.0	N/A	Goodman et al. [52]
CDI	NaCl 1169	561	1414	0.32	0.16-0.38	Hasseler et al. [41]
CDI	NaCl 1461-2922	731-2425	3792	0.8-1.9	0.19-0.39	Hand et al. [53]
MCDI	NaCl 1500	1000	379	N/A	0.13-0.30	Liu et al. [42]
MCDI	NaCl 1461-2922	731-2425	3792	0.4-0.9	0.25-1.75	Hand et al. [53]
MCDI	TDWW 1993 ^c	1241 ^c	$32^{\mathrm{b,d}}$	1.28 (1.05°)	1.07-1.58	This current study ^d
MCDI	TDWW 1993 ^c	1241 ^c	128 ^{b,f}	N/A	0.55-0.90	This current study ^f

BW: Brackish water, GW: Groundwater, TDWW: Treated domestic wastewater

^a Only RO pump power included.

^b Assuming 90 % production every day.

^c Assuming $TDS(mg/L) = 580 \times EC(mS/cm)$ (average ratio from historical water sampling at the Dubbo wastewater treatment plant).

^d Increased to a flowrate of product water for an 8-electrode module system.

 $^{^{\}rm e}\,$ Grid power requirement with photovoltaics powering the electrode modules.

f Increased to a flowrate of product water for a 32-electrode module system.

contribution of the electrodes to the overall power consumption to 0.72 kW (for 2 times the product) with the electrodes consuming 43 % of the input power. The MCDI system total energy requirement of 1.28 kWh/m 3 was within the reported range of reverse osmosis (RO) at 0.2 kWh/m 3 –1.9 kWh/m 3 and electrodialysis reversal (EDR) at 0.6 kWh/m 3 –2.67 kWh/m 3 (Table 3).

All of the cases where flowrate and applied current were varied involved the use of both mains and photovoltaics power supplies. No relationship was evident between flowrate or applied current and power consumption reduced by the use of photovoltaics. For the varying flowrate cases, the lowest power saving was in the 6.1 L/min case at 24 % savings and the highest saving was in the 6.9 L/min case with 43 % savings. As an absolute value, decreasing the flowrate resulted in a decrease in power saved from 0.42 kW in the 6.9 L/min case to 0.23 kW in the 3.8 L/min case. In the low flow cases, the pump power consumption decreased however the electrode power requirements also decreased as the cycle time reduced rendering the saving per product volume relatively constant. For the varying applied current cases, the lowest power saving occurred for the 100 A case at 22 % and the highest for the 120 A case at 28 % savings.

3.3.2. Effect of energy recovery

On average, 65 % of the available discharge energy was recovered with the energy recovery facility provided by the bidirectional charge/discharge current controllers ($\eta=0.65$) resulting in a 40 % reduction in the average electrode energy consumption. Due to resistance and losses within the system, the average voltage during discharging ($V_{avg,discharge}$) is lower than the average voltage during charging ($V_{avg,charge}$) (Fig. 2). As a result $E_{out} < E_{in}$ (refer Eqs. (5) and (6)) and so the portion of stored

charging energy recovered (40 %) is lower than the efficiency of the recovery (65 %) as outlined in Eq. (2). This is greater than results from a single electrode module unit where a maximum of 37.5 % energy reduction was achieved [22]. The maximum voltage used by Tan et al. [22] was 1.3 V whereas in this study, the maximum was set at 1.5 V. In this multi-module unit, the electrodes were operated in parallel so the current contribution from an electrode undergoing energy recovery during discharge is utilised by other charging electrodes. This reduces the RMS (root-mean-square) current in the batteries thereby reducing the loss associated with charge/discharge cycling (the roundtrip efficiency).

To estimate the benefit of coordinating the charge and discharge periods, two scenarios were considered i) with only one electrode module operating (Fig. 6a) and ii) with two electrodes operating in antiphase with coordinated charge and discharge stages synchronised appropriately (Fig. 6b, i.e. one charging and one discharging). From the single electrode study, a linear relationship was determined for the expected current draw from the 12 V battery compared to the electrode voltage during the charging phase (Supporting Information S6 Fig. S7). This can then be used to determine the difference between the expected current (Fig. 6a) and the actual current during the out of phase operation (Fig. 6b). The net current draw from the battery to the charging electrode is supplemented by the current returned from the discharging electrode, thereby lowering the current drawn from the battery. The variation between the electrode modules can be seen in Fig. 6b with electrode module 2 having a faster rate of change of voltage and subsequent shorter Δt_{cycle} than electrode module 1. This difference is likely due to variation between the internal resistances within the electrode modules and variation associated with particular installation issues such

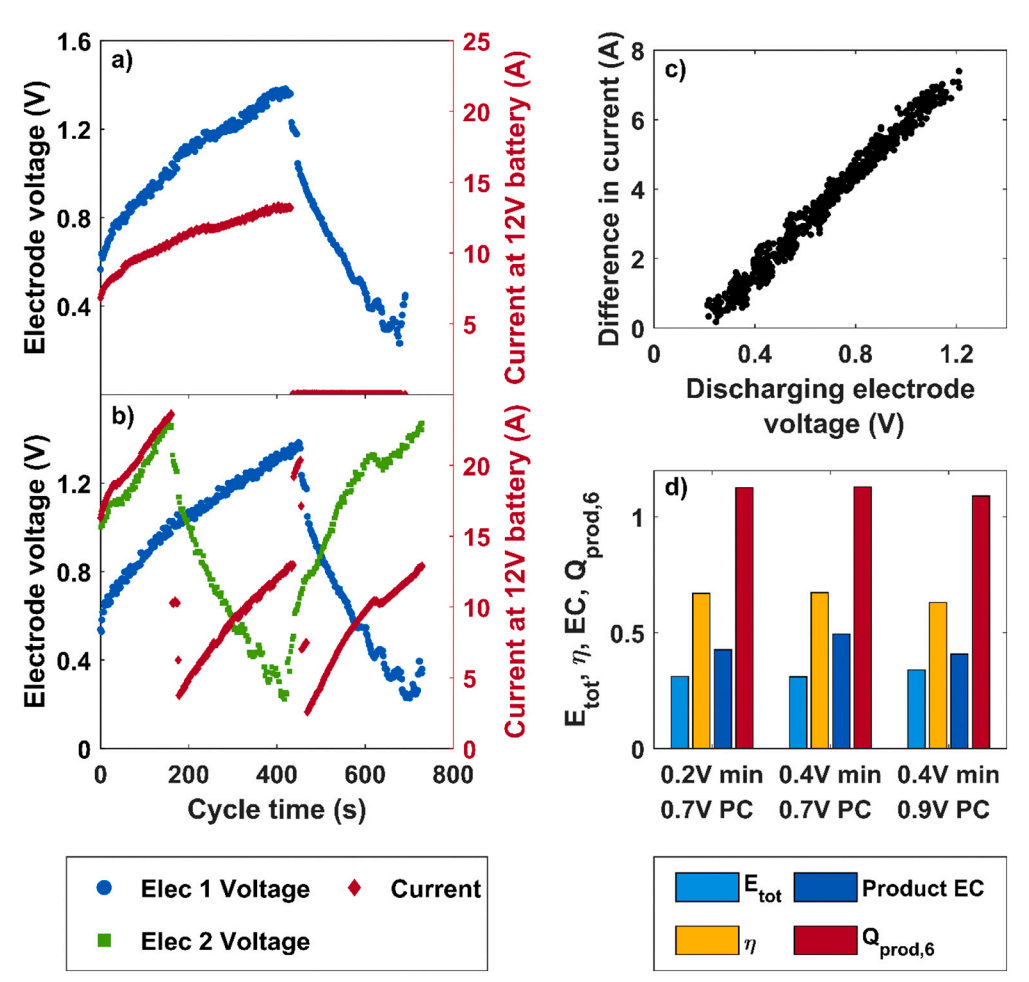


Fig. 6. a) Electrode voltage (V) and associated measured current at 12 V battery side (A) for a single electrode module operation. b) Electrode voltage (V) and associated measured current at 12 V battery side (A) for a dual electrode module operation, c) the difference between the expected current and the actual current at the battery side (A) versus the discharging electrode's voltage (V) (data collected over multiple cycles of single and dual electrode operation) and d) the measured electrode energy, E_{tot} (kWh/ m³), recovered portion of energy, η, product EC (mS/cm) and total flowrate of the product water for 6 electrode modules, Qprod.6 (m^3/h) for minimum discharge (V_{min}) of 0.2 V with a product collection cut off (PC) of 0.7 V, V_{min} of 0.4 V with a PC of 0.7 V and V_{min} of 0.4 V with a PC of 0.9 V. Note for a) the current transducer did not record negative current so this is shown as zero.

as hydraulic configuration and cable connections. A linear relationship between discharging electrode voltage and difference in current is evident (Fig. 6c), with approximately 0.25 V the lower limit for achievable energy recovery in this current scenario.

The higher the discharging electrode voltage, the higher the difference in current (Fig. 6c) indicating that to optimise for energy recovery, the discharge phase should stay at a high voltage. This can be achieved by increasing the minimum discharge voltage. This agrees with the observations of Tan et al. [22] who found that by increasing the minimum discharge voltage from 0.4 V to 0.8 V, the percentage of energy recovered increased from 27.5 % to 37.5 %. For this unit, average power consumption and η remained stable when the minimum discharge voltage was increased from 0.2 V to 0.4 V (Fig. 6d). However, with all settings the same, average product EC increased from $0.43\,\text{mS/cm}$ to $0.5\,$ mS/cm (Fig. 6d). The product collection cut off voltage level was increased from 0.7 V to 0.9 V to maintain product EC, however Q_{prod.6} dropped from 1.13 m³/h for the 6 electrode modules to 1.09 m³/h (Fig. 6d). Assuming an increase in minimum discharge voltage to say 0.6 V or 0.8 V will deliver additional energy reduction [22], the loss of either product quality or \mathbf{Q}_{prod} is not likely to be an acceptable trade off. It is therefore recommended to discharge to as low a discharge voltage as practical and forgo the energy loss by doing this.

By operating with higher discharge current and thereby reducing the discharge phase timing, η was reduced by 7 % (from 75 %, note that only 4 electrodes were operated for this comparison). Again, the operational optimisation needs to be balanced between Q_{prod} and $E_{tot}.$ Inclusion of the energy recovery device is recommended, as it enabled a 40 % energy saving on the electrode energy, despite longer cable runs and associated losses, with the inclusion of batteries also meaning that no heat sink device is needed and coupling to photovoltaics can be easily achieved.

3.4. Cost comparison

Capital costs for an eight-electrode module unit installed in late 2021 and currently operating in NT, Australia were used to enable comparison of costs between the operational scale MCDI system and RO and EDR (Table 3). The Q_{prod.1} of 0.17 m³/h from the MCDI unit described herein was used and multiplied by 8 with an engineering efficiency factor of 90 % [41,42]. The electrode module, flowmeter and EC sensors were given an estimated lifespan of five years and the lifespan of the remaining equipment was estimated at ten years. The capital cost for the MCDI system (not including interest) is \$1.07/m³. A grid electricity cost of \$0.20/kWh [43] and the sodium hypochlorite cleaning chemical and one hour per month of operator time at \$35/h equates to an operating cost of \$0.36/m3. This results in a total cost of water (not including interest) of \$1.33/m³ for the operational scale MCDI. When 5 % interest is in included, the levelized cost of water (LCOW) becomes \$1.58/m³. The container used for this trial would be able to fit 32 electrode modules. With 32 electrode modules, the cost of water (not including interest) would become \$0.55/m³ and the LCOW would become \$0.90/ m³. This is based on a grid electricity consumption equal to the eightelectrode module system of 1.05 kWh/m³ however, as mentioned in Section 3.3.1, as the system is scaled up, the contribution of the pumps would be expected to decrease, and this value would be expected to decrease. Cost estimations for such small scale systems are rarely reported, however the MCDI cost is within range of RO at \$0.19/m³ - $1.22/m^3$ and EDR at $1.02/m^3 - 5.29/m^3$ (Table 3).

4. Conclusions

An operational scale six electrode module MCDI desalination system was trialled at the Dubbo wastewater treatment plant to enable the plant to recycle water for screen cleaning. During the trial, no overall performance decline was noted in $\lambda,\,E_{tot}$ and WR despite operating for over 5000 cycles. Reverse current discharge operation and regular cleaning

with sodium hypochlorite solution were likely to have prevented biofilm growth as there was no pressure increase noted in the electrode modules despite a pressure increase across the 5 μm pre-filter. The unit was operated intermittently (i.e., usually turned off overnight) with no observable performance decline due to this intermittent operation. As MCDI operates with low pressure and has a low start up energy, intermittent operation can be easily achieved.

The operational scale multi-electrode module unit was found to demonstrate performance trends similar to bench scale MCDI systems with improved desalination performance as the flowrate decreases and the applied current increases. However, on transitioning from bench scale to operational scale MCDI units, maximum performance across all aspects may need to be compromised in order to enable appropriate operation of the system.

The use of photovoltaics for the electrode power supply resulted in an average power saving of 27 % compared to the case were mains only was used. The inclusion of energy recovery devices on the electrode control system enabled a 40 % reduction in electrode energy consumption compared to the case in which no energy was recovered. The inclusion of energy recovery with photovoltaics is recommended as the 12 V battery system needed to facilitate these aspects can be easily incorporated into MCDI systems.

Other system characteristics such as pH variation within the electrode during charging and discharging and release of divalent ions during discharging are areas of possible future work.

MCDI desalination was found to be a good solution when considering wastewater recycling as the system is able to run intermittently to accommodate supply requirements and has minimal cleaning requirements when operated in single pass mode. The cost and total system energy requirements were found to be within range of other more established water treatment technologies. It is a low pressure, low voltage technology with relatively lower energy start-stop cycles that make it well-suited to use with intermittent renewable power supplies. The system performance (such as energy consumption) has been shown to improve as the plant size increases, compared to technologies such as reverse osmosis, the process does not (unnecessarily) remove all constituents from the influent, and the operational range of the system is flexible as the process allows for selectivity, allowing for both a range of input qualities and desired outlet qualities.

Declaration of competing interest

The authors declare that they have no known competing financial interests or personal relationships that could have appeared to influence the work reported in this paper.

Data availability

Data will be made available on request.

Acknowledgements

The authors gratefully acknowledge Dubbo Regional Council for their assistance with the pilot plant placement, electricity supply, plumbing connections and ongoing support throughout the project. In particular we would like to acknowledge Hassan Badam, Max Newton, Rob Humphreys, Adam, and Quinton. The authors would like to express thanks to Calvin He for assistance with unit commissioning, Andrew Kinsela for his assistance with cation analysis and Yuyang Sun for his assistance with TOC analysis. Clare Bales gratefully acknowledges the Australian Government Research Training Program Scholarship, the UNSW Women in Engineering Research Top Up Scholarship (WIE) and the UNSW Engineering Supplementary Award (ESA).

CRediT authorship contribution statement

Clare Bales collected all the data, analysed this data and drafted the manuscript

Boyue Lian designed and installed the pilot MCDI unit and assisted in data collection

Yunyi Zhu assisted in data collection and interpretation of data Hang Zhou designed key electrical aspects of the pilot unit

Yuan Wang assisted in procurement of resources, partner relationships, project supervision and anuscript editing

John Fletcher assisted in procurement of resources, partner relationships, project supervision and manuscript editing

T. David Waite initiated the project and assisted in procurement of resources, partner relationships, project supervision and manuscript editing

Appendix A. Supplementary data

Supplementary data that includes details of the wastewater treatment plant and installed MCDI system, sample analysis methodology, filter and electrode module pressures and measured current under single electrode.to this article can be found online at https://doi.org/10.1016/j.desal.2023.116647.

References

- [1] F.A. Al Marzooqi, A.A. Al Ghaferi, I. Saadat, N. Hilal, Application of capacitive deionisation in water desalination: a review, Desalination 342 (2014) 3–15, https://doi.org/10.1016/j.desal.2014.02.031.
- [2] M.E. Suss, S. Porada, X. Sun, P.M. Biesheuvel, J. Yoon, V. Presser, Water desalination via capacitive deionization: what is it and what can we expect from it? Energy Environ. Sci. 8 (2015) 2296–2319, https://doi.org/10.1039/C5EE00519A.
- [3] S. Porada, R. Zhao, A. van der Wal, V. Presser, P.M. Biesheuvel, Review on the science and technology of water desalination by capacitive deionization, Prog. Mater. Sci. 58 (2013) 1388–1442, https://doi.org/10.1016/j.pmatsci.2013.03.005.
- [4] P.M. Biesheuvel, A. van der Wal, Membrane capacitive deionization, J. Membr. Sci. 346 (2010) 256–262, https://doi.org/10.1016/j.memsci.2009.09.043.
- [5] R. Zhao, P.M. Biesheuvel, A. van der Wal, Energy consumption and constant current operation in membrane capacitive deionization, Energy Environ. Sci. 5 (2012) 9520–9527, https://doi.org/10.1039/c2ee21737f.
- [6] P.M. Biesheuvel, R. Zhao, S. Porada, A. van der Wal, Theory of membrane capacitive deionization including the effect of the electrode pore space, J. Colloid Interface Sci. 360 (2011) 239–248, https://doi.org/10.1016/j.jcis.2011.04.049.
- [7] J.B. Lee, K.K. Park, H.M. Eum, C.W. Lee, Desalination of a thermal power plant wastewater by membrane capacitive deionization, Desalination 196 (2006) 125–134, https://doi.org/10.1016/j.desal.2006.01.011.
- [8] W. Tang, D. He, C. Zhang, P. Kovalsky, T.D. Waite, Comparison of faradaic reactions in capacitive deionization (CDI) and membrane capacitive deionization (MCDI) water treatment processes, Water Res. 120 (2017) 229–237, https://doi. org/10.1016/J.WATRES.2017.05.009.
- [9] D.I. Kim, P. Dorji, G. Gwak, S. Phuntsho, S. Hong, H. Shon, Reuse of municipal wastewater via membrane capacitive deionization using ion-selective polymercoated carbon electrodes in pilot-scale, Chem. Eng. J. 372 (2019) 241–250, https://doi.org/10.1016/j.cej.2019.04.156.
- [10] Y.Y. Shen, S.H. Sun, S.W. Tsai, T.H. Chen, C.H. Hou, Development of a membrane capacitive deionization stack for domestic wastewater reclamation: a pilot-scale feasibility study, Desalination 500 (2021), 114851, https://doi.org/10.1016/j. desal.2020.114851.
- [11] C. Feng, C.C. Tsai, C.Y. Ma, C.P. Yu, C.H. Hou, Integrating cost-effective microbial fuel cells and energy-efficient capacitive deionization for advanced domestic wastewater treatment, Chem. Eng. J. 330 (2017) 1–10, https://doi.org/10.1016/j. cei.2017.07.122.
- [12] M. Lee, C.S. Fan, Y.W. Chen, K.C. Chang, P. Te Chiueh, C.H. Hou, Membrane capacitive deionization for low-salinity desalination in the reclamation of domestic wastewater effluents, Chemosphere 235 (2019) 413–422, https://doi.org/10.1016/j.chemosphere.2019.06.190.
- [13] Z. Ge, X. Chen, X. Huang, Z.J. Ren, Capacitive deionization for nutrient recovery from wastewater with disinfection capability, Environ. Sci. Water Res. Technol. 4 (2018) 33–39, https://doi.org/10.1039/c7ew00350a.
- [14] Y. Bian, X. Chen, L. Lu, P. Liang, Z.J. Ren, Concurrent nitrogen and phosphorus recovery using flow-electrode capacitive deionization, ACS Sustain. Chem. Eng. 7 (2019) 7844–7850, https://doi.org/10.1021/acssuschemeng.9b00065.
- [15] O. Pastushok, F. Zhao, D.L. Ramasamy, M. Sillanpää, Nitrate removal and recovery by capacitive deionization (CDI), Chem. Eng. J. 375 (2019), 121943, https://doi. org/10.1016/j.cej.2019.121943.
- [16] F.F. Chen, H.F. Li, X.R. Jia, Z.Y. Wang, X. Liang, Y.Y. Qin, W.Q. Chen, T.Q. Ao, Characteristic and model of phosphate adsorption by activated carbon electrodes

- in capacitive deionization, Sep. Purif. Technol. 236 (2020), 116285, https://doi.org/10.1016/j.seppur.2019.116285.
- [17] J. Jiang, D.I. Kim, P. Dorji, S. Phuntsho, S. Hong, H.K. Shon, Phosphorus removal mechanisms from domestic wastewater by membrane capacitive deionization and system optimization for enhanced phosphate removal, Process Saf. Environ. Prot. 126 (2019) 44–52, https://doi.org/10.1016/j.psep.2019.04.005.
- [18] C. Zhang, J. Ma, D. He, T.D. Waite, Capacitive membrane stripping for ammonia recovery (CapAmm) from dilute wastewaters, Environ. Sci. Technol. Lett. 5 (2018) 43–49, https://doi.org/10.1021/acs.estlett.7b00534.
- [19] A. Hassanvand, G.Q. Chen, P.A. Webley, S.E. Kentish, An investigation of the impact of fouling agents in capacitive and membrane capacitive deionisation, Desalination 457 (2019) 96–102, https://doi.org/10.1016/j.desal.2019.01.031.
- [20] P. Długolęcki, A. Van Der Wal, Energy recovery in membrane capacitive deionization, Environ. Sci. Technol. 47 (2013) 4904–4910, https://doi.org/ 10.1021/es3053202
- [21] J. Kang, T. Kim, H. Shin, J. Lee, J.-I. Ha, J. Yoon, Direct energy recovery system for membrane capacitive deionization, Desalination 398 (2016) 144–150, https://doi. org/10.1016/j.desal.2016.07.025.
- [22] C. Tan, C. He, J. Fletcher, T.D. Waite, Energy recovery in pilot scale membrane CDI treatment of brackish waters, Water Res. 168 (2020), 115146, https://doi.org/ 10.1016/j.watres.2019.115146
- [23] C. Tan, C. He, W. Tang, P. Kovalsky, J. Fletcher, T.D. Waite, Integration of photovoltaic energy supply with membrane capacitive deionization (MCDI) for salt removal from brackish waters, Water Res. 147 (2018) 276–286, https://doi.org/ 10.1016/j.watres.2018.09.056.
- [24] W. Zhang, M. Mossad, J.S. Yazdi, L. Zou, A statistical experimental investigation on arsenic removal using capacitive deionization, Desalin. Water Treat. 57 (2016) 3254–3260, https://doi.org/10.1080/19443994.2014.981761.
- [25] L. Chen, C. Wang, S. Liu, Q. Hu, L. Zhu, C. Cao, Investigation of the long-term desalination performance of membrane capacitive deionization at the presence of organic foulants, Chemosphere 193 (2018) 989–997, https://doi.org/10.1016/j. chemosphere.2017.11.130.
- [26] C. Wang, L. Chen, L. Zhu, Effect of combined fouling on desalination performance of membrane capacitive deionization (MCDI) during long-term operation, J. Dispers. Sci. Technol. 41 (2019) 383–392, https://doi.org/10.1080/ 01932691.2019.1579654.
- [27] J. Yu, K. Jo, T. Kim, J. Lee, J. Yoon, Temporal and spatial distribution of pH in flow-mode capacitive deionization and membrane capacitive deionization, Desalination 439 (2018) 188–195, https://doi.org/10.1016/j.desal.2018.04.011.
- [28] W. Zhang, M. Mossad, L. Zou, A study of the long-term operation of capacitive deionisation in inland brackish water desalination, Desalination 320 (2013) 80–85, https://doi.org/10.1016/j.desal.2013.04.010.
- [29] WaterNSW, Continuous water monitoring network. https://realtimedata.waterns w.com.au/, 2023 (accessed January 4, 2023.
- [30] H. Zhou, C. Tan, J. Fletcher, Lossless bi-directional current sense circuit for low-voltage high-current DC/DC converters, in: Proc. IECON 2018 44th Annu. Conf. IEEE Ind. Electron. Soc, 2018, pp. 1305–1308, https://doi.org/10.1109/IECON 2018 8591710
- [31] Dubbo Regional Council, Water Quality and Treatment Drinking Water Quality. https://www.dubbo.nsw.gov.au/our-region-and-environment/water-sewe rage-and-drainage/water-quality-treatment/water-quality-and-treatment, 2020 (accessed August 14, 2020).
- [32] B. Lian, Y. Zhu, D. Branchaud, Y. Wang, C. Bales, T. Bednarz, T.D. Waite, Application of digital twins for remote operation of membrane capacitive deionization (mCDI) systems, Desalination 525 (2022), https://doi.org/10.1016/j. desal.2021.115482.
- [33] S.A. Hawks, A. Ramachandran, S. Porada, P.G. Campbell, M.E. Suss, P. M. Biesheuvel, J.G. Santiago, M. Stadermann, Performance metrics for the objective assessment of capacitive deionization systems, Water Res. 152 (2019) 126–137, https://doi.org/10.1016/j.watres.2018.10.074.
- [34] M.A. Anderson, A.L. Cudero, J. Palma, Capacitive deionization as an electrochemical means of saving energy and delivering clean water. Comparison to present desalination practices: will it compete? Electrochim. Acta 55 (2010) 3845–3856, https://doi.org/10.1016/j.electacta.2010.02.012.
- [35] EWT Water Technology, Concentration Quantities and Unit Conversions in Water Chemistry, 2018 (accessed March 27, 2020), http://www.ewt-wasser.de/en/kn owledge/concentration-quantities-unit-conversions.html.
- [36] R. Zhao, S. Porada, P.M. Biesheuvel, A. van der Wal, Energy consumption in membrane capacitive deionization for different water recoveries and flow rates, and comparison with reverse osmosis, Desalination 330 (2013) 35–41, https://doi. org/10.1016/j.desal.2013.08.017.
- [37] R. Zhao, O. Satpradit, H.H.M. Rijnaarts, P.M. Biesheuvel, A. van der Wal, Optimization of salt adsorption rate in membrane capacitive deionization, Water Res. 47 (2013) 1941–1952, https://doi.org/10.1016/j.watres.2013.01.025.
- [38] Y.A.C. Jande, W.S. Kim, Desalination using capacitive deionization at constant current, Desalination 329 (2013) 29–34, https://doi.org/10.1016/j. desal.2013.08.023.
- [39] Y. Zhu, B. Lian, Y. Wang, C. Miller, C. Bales, J. Fletcher, L. Yao, T.D. Waite, Machine learning modelling of a membrane capacitive deionization (MCDI) system for prediction of long-term system performance and optimization of process control parameters in remote brackish water desalination, Water Res. 227 (2022), 119349, https://doi.org/10.1016/j.watres.2022.119349.
- [40] T. Luo, S. Abdu, M. Wessling, Selectivity of ion exchange membranes: a review, J. Membr. Sci. 555 (2018) 429–454, https://doi.org/10.1016/j. memsci.2018.03.051.

- [41] T.D. Hasseler, A. Ramachandran, W.A. Tarpeh, M. Stadermann, J.G. Santiago, Process design tools and techno-economic analysis for capacitive deionization, Water Res. 183 (2020), 116034, https://doi.org/10.1016/j.watres.2020.116034.
- [42] X. Liu, S. Shanbhag, T.V. Bartholomew, J.F. Whitacre, M.S. Mauter, Cost comparison of capacitive deionization and reverse osmosis for brackish water desalination, ACS ES&T Eng. 1 (2020) 261–273, https://doi.org/10.1021/ acsestenge.0C00094.
- [43] K. Wrigley, Average Electricity Prices in Australia per kWh. https://www.canst arblue.com.au/electricity/electricity-costs-kwh/, 2023 (accessed February 14, 2023).
- [44] M.A. Alghoul, P. Poovanaesvaran, M.H. Mohammed, A.M. Fadhil, A.F. Muftah, M. M. Alkilani, K. Sopian, Design and experimental performance of brackish water reverse osmosis desalination unit powered by 2 kW photovoltaic system, Renew. Energy 93 (2016) 101–114, https://doi.org/10.1016/j.renene.2016.02.015.
- [45] M.A. Hafiz, A.H. Hawari, R. Alfahel, M.K. Hassan, A. Altaee, Comparison of nanofiltration with reverse osmosis in reclaiming tertiary treated municipal wastewater for irrigation purposes, Membranes (Basel) 11 (2021) 32, https://doi. org/10.3390/membranes11010032.
- [46] B. Peñate, V.J. Subiela, F. Vega, F. Castellano, F.J. Domínguez, V. Millán, Uninterrupted eight-year operation of the autonomous solar photovoltaic reverse osmosis system in Ksar Ghilène (Tunisia), Desalin. Water Treat. 55 (2014) 3141–3148, https://doi.org/10.1080/19443994.2014.940643.
- [47] A. Alsarayreh, M. Majdalawi, R. Bhandari, Techno-economic study of PV powered brackish water reverse osmosis desalination plant in the Jordan Valley, Int. J. Therm. Environ. Eng. 14 (2017) 83–88, https://doi.org/10.5383/ijtee.14.01.010.

- [48] P. Kehrein, M. Jafari, M. Slagt, E. Cornelissen, P. Osseweijer, J. Posada, M. van Loosdrecht, A techno-economic analysis of membrane-based advanced treatment processes for the reuse of municipal wastewater, J. Water Reuse Desalin. 11 (2021) 705–725, https://doi.org/10.2166/wrd.2021.016.
- [49] F. Vince, F. Marechal, E. Aoustin, P. Bréant, Multi-objective optimization of RO desalination plants, Desalination 222 (2008) 96–118, https://doi.org/10.1016/j.desal.2007.02.064
- [50] D.W. Bian, S.M. Watson, N.C. Wright, S.R. Shah, T. Buonassisi, D. Ramanujan, I. M. Peters, A.G. Winter, Optimization and design of a low-cost, village-scale, photovoltaic-powered, electrodialysis reversal desalination system for rural India, Desalination 452 (2019) 265–278, https://doi.org/10.1016/j.desal.2018.09.004.
- [51] W. He, S. Amrose, N.C. Wright, T. Buonassisi, I.M. Peters, A.G. Winter, Field demonstration of a cost-optimized solar powered electrodialysis reversal desalination system in rural India, Desalination 476 (2020), 114217, https://doi. org/10.1016/j.desal.2019.114217.
- [52] N.B. Goodman, R.J. Taylor, Z. Xie, Y. Gozukara, A. Clements, A feasibility study of municipal wastewater desalination using electrodialysis reversal to provide recycled water for horticultural irrigation, Desalination 317 (2013) 77–83, https://doi.org/10.1016/j.desal.2013.02.010.
- [53] S. Hand, J.S. Guest, R.D. Cusick, Technoeconomic analysis of brackish water capacitive deionization: navigating tradeoffs between performance, lifetime, and material costs, Environ. Sci. Technol. 53 (2019) 13353–13363, https://doi.org/ 10.1021/acs.est.9b04347.